

Uhriumov Yu.D., Dobriak V.D., Mazur I.A., Uhriumov D.Yu.
Preparation of rolled products for processing at a pipe rolling unit
Угрюмов Ю.Д., Добряк В.Д., Мазур І.А., Угрюмов Д.Ю.
Підготовка розкату по переділах трубопрокатного агрегата

Abstract. Purpose. The aim of this work is to examine rolling processes with variable deformation modes by transferring part of this deformation from the mill under consideration to the preceding mill, as well as to develop a process for preparing the billet ends by transverse planetary burnishing with idle rolls. **Methodology.** Using the slip-line method, the forces acting on the idle rolls during transverse planetary burnishing of the billet end, as well as the torque and power of the burnishing process, were determined. The thinning of the wall at the front end of the billet during its preparation by transverse planetary burnishing with idle rolls was analytically established. **Findings.** One of the main reserves for further increasing productivity, saving metal, and improving geometric dimensions in the production of hot-rolled seamless pipes is the use of variable deformation modes across the wall thickness. Examples of additional operations carried out on various pipe-rolling mills are considered, demonstrating their high efficiency. For the design of a method for preparing the front ends of billets, planetary rolling processes applied in pipe-rolling production were analyzed. **Originality.** The method of transferring part of the deformation from the main mill to the preceding mill has been further developed, which significantly improves rolling conditions in the main mill and enhances its performance indicators. **Practical value.** The process of transverse planetary burnishing of billet ends appears highly promising and warrants further research and development. The results of this work can be applied in selecting the most rational method of metal preparation for rolling, taking into account the specific technology of a given pipe-rolling mill.

Key words: hot-rolled pipe, pipe-rolling mill, billet, mandrel, plug, end preparation, skew rolling piercer, transverse planetary burnishing, slip-line method, rolling force, rolling torque, rolling power, productivity.

Анотація. Мета. Метою цієї роботи є дослідження процесів прокатки зі змінними режимами деформації шляхом передачі частини цієї деформації з розглянутого стану на попередній, а також розробка процесу підготовки торців заготовок поперечним планетарним вигладжуванням холостими валками. **Методика.** За допомогою методу ковзання визначалися сили, що діють на холості валки під час поперечного планетарного вигладжування торця заготовки, а також крутний момент і потужність процесу вигладжування. Аналітично встановлено стоншення стінки на передньому кінці заготовки під час її підготовки поперечним планетарним вигладжуванням холостими валками. **Результатами.** Одним з основних резервів подальшого підвищення продуктивності, економії металу та покращення геометрических розмірів у виробництві гарячекатаних безшових труб є використання змінних режимів деформації по товщині стінки. Розглянуто приклади додаткових операцій, що виконуються на різних трубопрокатних станах, що демонструють їх високу ефективність. Для розробки методу підготовки передніх торців заготовок проаналізовано процеси планетарної прокатки, що застосовуються в трубопрокатному виробництві. **Оригінальність.** Розроблено метод передачі частини деформації з основного стану на попередній, що значно покращує умови прокатки в основному стані та підвищує його продуктивні показники. **Практична цінність.** Процес поперечного планетарного вигладжування торців заготовок є дуже перспективним і потребує подальших досліджень і розробок. Результатами цієї роботи можуть бути застосовані при виборі найбільш раціонального методу підготовки металу до прокатки з урахуванням специфіки технології даного трубопрокатного стану.

Ключові слова: гарячекатана труба, трубопрокатний стан, заготовка, оправка, пробка, підготовка торців, косопрокатний пробивний стан, поперечне планетарне вигладжування, метод ковзання, сила прокатки, крутний момент прокатки, сила прокатки, продуктивність.

Introduction. The production of hot-rolled seamless pipes of a wide dimensional and grade range is carried out on various pipe-rolling mills (PRMs), the characteristics of which are defined by the main rolling mill, which deforms the billet on a mandrel into a rough pipe. Different types of rolling mills are known, including pilger mills, continuous mills, automatic mills, Assel three-roll mills, rail mills, Disher mills, and others [1]. The bulk of hot-rolled pipe production is performed on PRMs equipped with pilger, continuous, automatic, and Assel three-roll mills.

One of the principal directions in the advancement of metallurgy worldwide is resource conservation and

environmental protection [1], which necessitates the improvement of existing technological processes as well as the creation of new ones, in line with scientific and technological progress. Due to intense competition in global pipe markets, the key indicators of production efficiency are competitive cost and product quality.

Studies conducted in [2] have shown that one of the main reserves for further increasing productivity, saving metal, and improving dimensional accuracy in the production of hot-rolled seamless pipes is the use of variable deformation regimes across the wall thickness. In particular, variation of wall thickness along the



pipe length in mills incorporated into PRMs of different types can be realized either by adjusting the roll gap or by shifting the mandrel during rolling. The method of transferring part of the deformation from the main mill to the preceding mill has been further developed, which significantly improves rolling conditions in the main mill and enhances its performance indicators. Examples of such technology include various operations for preparing the front and rear ends of billets and shells prior to pipe rolling.

In general, the technological process in a PRM consists of four production modules (fig. 1): module 1 – metal preparation for rolling; module 2 – billet piercing to obtain a hollow shell; module 3 – rolling of the rough pipe; module 4 – production of the finished pipe.

Each module includes the following main operations:

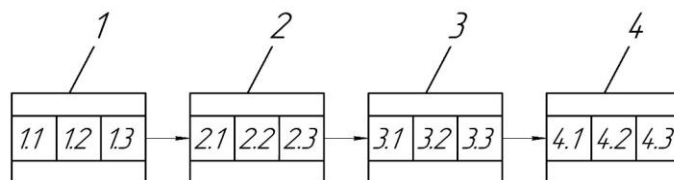


Figure 1 – Generalized technological scheme of pipe production on PRM of various types.

Features of pipe production on different PRMs [1]. The process of producing pipes on PRMs with pilger mills has gained widespread use worldwide for manufacturing pipes with outer diameters ranging from 60 mm to 800 mm, which is determined by the roll diameters of the pilger mill. These units allow the production of pipes from various types of initial billets, including ingots from stationary casting, continuously cast billets (CCB), as well as centrifugally cast, rolled, forged, and other billets. One of the advantages of producing pipes on these PRMs is the possibility of obtaining thick-

walled pipes of considerable length, as well as profiled pipes made from various steels and alloys. On PRMs with pilger mills, it is economically feasible to produce both small and large batches of pipes. At the same time, this process is characterized by increased metal consumption due to technologically unavoidable losses in the final trim: the starter and pilger head.

The average value of the metal consumption coefficient (MCC) for hot-rolled oil pipelines and general-purpose pipes, according to SE "UkrDIPROMEZ" is presented in table 1.

Table 1 – MCC (t/t) for hot-rolled oil pipeline and general-purpose pipes on different types of PRMs

Type of pipes	With automatic mill «140»	With Pilger mill	With three-roll rolling mill	With continuous mill «30-102»
Carbon	1,067–1,083	1,20	1,060	1,066–1,077
Alloyed	1,087–1,103	1,24	1,080	1,087–1,091
High-alloy	1,107	1,32	1,100	–

According to the data presented in table 1, the highest metal losses are observed on PRMs with pilger mills, which is associated with the presence of the starter and pilger head, which are removed during rolling. In this case, metal losses in the starter account for 20–25%, and in the pilger head 75–80% of the total technological trim on the pilger mill. The main metal loss in the trim occurs during the rolling of thin-walled $\frac{D}{S} = 12,5 \div 40,0$ and extra-thin-walled $\frac{D}{S} > 40,0$ pipes.

On PRMs with Assel three-roll mills, pipes are obtained with a ratio $\frac{D}{S} < 11,0$, that results in an MCC value significantly lower than on PRMs with pilger mills. These pipes are mainly used as billets for the production of ball bearings.

PRMs with automatic mills have gained the widest global use due to their versatility in producing pipes of a wide range of sizes and grades. They are economically feasible for rolling both large and small batches of pipes. The MCC values on these PRMs are comparable to those on continuous mills and three-roll mills.

Over the last 50 years, PRMs with continuous mills have experienced the greatest development worldwide due to their high productivity, high pipe quality, and degree of automation. They are used to produce high-precision pipes with diameters up to 426 mm.

Increased metal losses during pipe production on PRMs with automatic and continuous mills occur when using the pipe reducing technology with stretching, which leads to increased trimming of thickened pipe ends.

Problem statement. Further improvement of the hot-rolled seamless pipe production process to enhance its technical and economic performance is associated with the use of variable deformation modes by adjusting the main rolling parameters, as well as by transferring part of the deformation from the main mill to the preceding mill.

Aim and objectives of the research. The aim of this work is to consider the second approach, analyze solutions for preparing the ends of the billet on different PRM mills, and develop a process for preparing billet ends using planetary rolling with idle rolls.

Research results. To improve the hot-rolled pipe production process on different types of PRMs, it is advisable to perform additional operations on the

preceding mill to reduce deformations on the mill under consideration. A structural diagram of the main operations on the PRM is shown in fig. 2. The main operations include the following: 1 – preparation of the billet for piercing on a skew-roll mill; 2 – piercing of the billet into a shell on the skew-roll mill; 3 – rolling of the shell into a rough pipe (first pass); 4 – rolling of the rough pipe (second pass); 5 – production of the finished pipe.

Let us consider the use of additional operations performed on the preceding mill to improve the rolling process on the main (subsequent) mill. The additional operations listed are not exhaustive, as the number of such operations is quite large. New additional operations allow the expansion of the structural diagram presented in fig. 2.

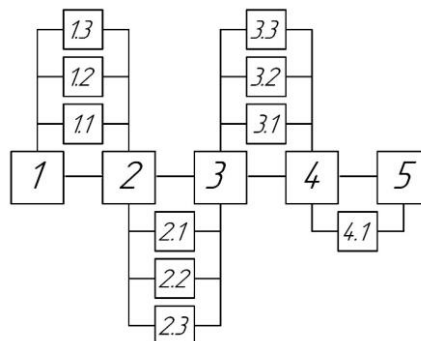


Figure 2 – Structural diagram of the main operations on the PRM with metal preparation in preceding operations

Preparation of the billet for piercing on the skew-roll mill: 1.1 – profiling of the ends and centering of the billet faces; 1.2 – preliminary upsetting of the CCB on the radial-shear rolling mill (RSR); 1.3 – profiling of the cylindrical surface of the billet.

Piercing of the billet into a shell on the skew-roll mill: 2.1 – preparation (profiling) of the shell ends; 2.2 – preparation of the rear ends of the shells; 2.3 – obtaining shells with longitudinal wall thickness variation.

Rolling of the shell into a rough pipe (first pass): 3.1 – rolling of the pipe with thinned ends on the pilger mill; 3.2 – thinning of the front ends of the pipes on the automatic mill; 3.3 – thinning of the pipe ends on the continuous mill.

Rolling of the rough pipe (second pass): 4.1 – changing the roll gap of the rolling mill along the pipe length.

Let us consider examples of performing additional operations (positions 1.1–1.3, fig. 2) to improve the piercing of the billet on the skew-roll mill.

The process of filling and releasing the deformation zone during skew-roll piercing is accompanied by intensive transverse deformation of the front and rear ends of the billet. This is explained by the absence, during these periods of the process, of so-called «rigid ends» that restrain transverse deformation. As a result, axial drawing occurs at the front and rear faces, the magnitude of which depends on the upsetting and the number of deformation cycles. At the end of the piercing process, the number of deformation cycles of the

metal in front of the mandrel tip increases, raising the likelihood of opening the axial cavity. The formation of such a cavity leads to internal defects at the ends of the shells and pipes.

Studies [3, 4] have shown that profiling the front and rear ends of billets with a spherical convex surface allows the introduction of the necessary metal volume for the mandrel tip, which acts as a «rigid end» and restrains transverse metal deformation. This improves gripping conditions, reduces the number of deformation cycles, decreases axial drawing, increases the accuracy of the shell and pipe ends, and reduces the number of internal end laps [5]. It should be noted that such preparation of billet ends in the PRM line is problematic without introducing an additional operation and installing the corresponding equipment. This can be considered a factor limiting the implementation of such a billet-end preparation process in production. A known proposal for preparing the rear ends of billets during piercing on the skew-roll mill [6] involves initially centering the front end of the billet while supporting the rear end with an additional centering head, and centering the rear end of the billet at the moment it enters the piercing roll gap. This method of billet preparation allows increasing the processing accuracy of the resulting products by eliminating misalignment between the billet and the piercing axis. To center the axial drawing at the rear end, the centering head is pressed with a force that prevents it from pushing out of the drawing and moves at the same speed as the billet end. This

method improves the accuracy of the pierced product ends and, consequently, reduces metal consumption due to technological trimming.

At «UralNDTI», it was proposed to pierce billets with a wavy profile on the lateral surface [7]. The intermittent contact of the metal with the rolls and the fine deformation significantly reduce the negative influence of frictional backing forces, creating conditions for predominant metal flow in the axial direction. Experimental studies on piercing billets with a wavy profile demonstrated an increase in the critical upsetting by 2,8÷4,0 times and a reduction of the energy-force parameters of the piercing process by 18÷30% compared to the existing parameters for piercing cylindrical billets [7].

Let us consider examples of performing additional operations (positions 2.1–2.3, fig. 2) to improve the rolling of the rough pipe (first pass). To enhance hot pilger pipe rolling in the unstable «starter» mode, the preparation of the front ends of shells is known to be applied [8]. Improvement of the starter mode conditions occurs due to the transfer of part of the metal deformation to the preceding mill, for example, the piercing mill. This allows reducing metal losses in the trim at the front (starter) end of the pipe and shortening the duration of the starter mode, thereby increasing the productivity of the pilger mill.

Expansion of the size range at the stage of increasing $\frac{D}{S}$ the pipes rolled on PRMs with Assel three-roll mills is achieved by thinning the rear end of the shell during its piercing on the skew-roll mill. Reducing deformation when rolling the rear ends of shells on the Assel three-roll mill decreases transverse deformation, which allows rolling the main part of the pipe with a thinner wall [9].

On PRMs with the automatic mill 350, a new rolling technology has been developed and implemented, which reduces longitudinal wall thickness variation of pipes, averaging 0,2÷0,5 mm. This variation is primarily caused by temperature differences along the length of the shell formed during billet piercing, which induces changes in the elastic deformation of the automatic mill working stand. The new technology [10] involves rolling shells on the piercing mill with wall thickness increasing from the front to the rear end by expanding the rolls during piercing. During subsequent rolling of these shells on the automatic mill, increasing billet compression compensates for the temperature gradient along the shell, stabilizing roll forces and the gap between them.

To implement the piercing process, a tensioning device equipped with a program-controlled automatic system was developed. The system ensures the specified radial displacement of the rolls. Reducing longitudinal wall thickness variation allowed a decrease in average wall thickness by 0,044 mm, correspondingly reducing metal consumption by 5 kg per ton of finished pipe.

Let us consider examples of performing additional operations (positions 3.1–3.3, fig. 2) to improve the rough pipe rolling (second pass).

A known technology [11] involves rolling pipes on the pilger mill with thickened ends corresponding to the starter end and the pilger head. By reducing metal deformation, metal losses in the starter end and pilger head are significantly reduced. In addition, this ensures the removal of the pipe from the mandrel during rolling of thin-walled pipes with $\frac{D}{S} = 12,5 \div 40,0$.

The preparation of pipe billets for reducing on the preceding stages of the technological process has been considered in works [12, 13] and others. One of the main approaches to reducing metal waste during hot pipe reducing is to vary the deformation along the pipe length. In this case, deformation is redistributed between two stages of the technological process: in the part of the pipe where the required degree of deformation cannot be achieved in the reducing mill, it is increased at the preceding PRM stage.

The most effective method realizing this approach is to change the deformation zone by converging or diverging the working rolls directly during pipe rolling. Two methods of implementing this approach are known: on existing equipment outside or in addition to the main technological process, and on existing equipment within the normal technological flow.

On PRMs with the automatic mill 140, when rolling rough pipes with diameters of 84÷118 mm and wall thicknesses of 3,4÷12 mm, their ends were thinned over a length of 600÷1800 mm, with additional wall compression at the ends of 0,25÷1,0 mm. During subsequent reducing with stretching into pipes with diameters of 28÷76 mm and wall thicknesses of 3,2÷12 mm, a metal saving of 900 t/year was achieved. The increase in length of the reduced and calibrated pipes was within 2,7÷5,4% and 2,8÷4,6%, respectively, and metal savings were also achieved due to reducing the billet length when rolling pipes of measured length by 5% [14].

Let us consider an example of performing an additional operation (position 4.1, fig. 2).

On PRMs with the automatic mill 350, the transverse wall thickness variation of the pipe ΔS_k end sections is 1,5÷2,0 times greater than the variation in their middle section. M.I. Khanin proposed that, to utilize the tolerance range of thickened pipe ends on PRMs with automatic mill 350, the wall thickness of the pipe should be adjusted at the final stage of its shaping on the rolling mill [15].

For this purpose, during the rolling of the pipe end sections, it is necessary to change the distance between the rolls: the rolls are converged at the front end of the pipe and diverged at the rear end. It is advisable to implement roll displacement during rolling using the pressure device of the rolling mill. The rolling technology on the rolling mill is as follows [15]. After the front end of the pipe exits the rolls by 0,4÷0,6 m, the rolls are converged by a specified amount using the mill's pressure device, increasing wall compression by $\Delta = 0,1 \div 0,3$ mm. The middle section of the pipe is rolled at a constant distance between the rolls, which differs from the initial distance by the amount of their convergence.

As the rear end of the pipe approaches the deformation zone, the rolls are diverged back to their original position. The completion of roll divergence should correspond to a distance of 0,4÷0,6 m from the rear pipe end to the deformation zone. The rear end of the pipe is rolled according to the mill setting specified in the rolling schedule. Roll movement during rolling should be performed in automatic mode.

Methods for preparing the front ends of shells before rolling. These methods are discussed in detail in [8]. Preparation of the front ends of shells is known primarily on the skew-roll piercing mill and in the off-line charging section of the pilger mill. The most rational method for preparing shell ends on the piercing mill is compression using idle rolls at the exit side of the stand on the mandrel, utilizing the forces of the piercing process. Studies of this process on PRMs with pilger mills at 6 – 12" i 5 – 12" and at PJSC «Interpipe-NTZ» showed its high efficiency, increasing the productivity of the pilger mill by 3÷4% and reducing metal consumption by 1,5÷2,5%. Examples of preparing the front ends of shells in the off-line charging section of the pilger mill include deformation of the shell front end on a temporary mandrel using a four-ram hydraulic press and on a planetary-type rolling machine. The most promising direction is the use of planetary skew-roll (transverse) mills. In planetary skew-roll mills, the rolls rotate planetarily around a stationary billet, continuously deforming it in a steady-state mode. Further research on the process of skew-roll (transverse) planetary rolling is necessary for the preparation of the front ends of shells.

Planetary rolling processes in pipe production. Let us consider the main directions of using the planetary rolling process by deforming metal in idle rolls located in a cassette that rotates.

Rolling in three-roll (PSW) and four-roll (KRM) planetary mills [1]. Planetary skew-roll mills differ from traditional screw rolling mills in that the work stand with rolls rotates around the pipe, rather than the pipe itself rotating. Rolling in a rotating stand was first used to produce rods and pipes of a wide range of grades from

non-ferrous metals. The production of seamless pipes was initiated on the PSW mill in 1974. On the PSW mill, pipes with an outer diameter of 70–219 mm and wall thickness of 4,5–6,0 mm are produced, with a ratio of $\frac{D}{S} = 8 \div 35$. The elongation coefficient can reach $\mu = 15$.

The company «KOCKS» developed a «new» technology for producing seamless pipes through a continuous process of transforming a hollow billet into a hot-rolled pipe (STP process), which uses a four-roll elongator (KRM) whose rolls rotate around the billet. As a result, the KRM mill is capable of rolling shells (rough pipes) up to 50 m in length. While the rear part of the hollow billet is transformed into a shell on the KRM mill, the front part begins forming into the finished pipe in the reducing-elongation mill. The reducing-elongation mill, equipped with adjustable stands, is a continuation of developments of traditional PPC mills, based on the positive experience of three-roll reducing and calibrating mills used for rolling wire and rods, and meets the requirements of the pipe market.

Elongation in the KRM mill, reduction in the reducing-elongation mill, and cutting of pipes on a flying saw occur simultaneously on the same billet, eliminating additional heating. This technology increases profitability and productivity while also expanding the pipe assortment.

1. The use of planetary skew-roll mills as expansion stands is known [16].

2. The principle of planetary rolling was applied in [17] for developing a method for preparing the front ends of shells before pilger rolling. In the proposed process (fig. 3), preparation of the shell end is performed on a temporary short cylindrical mandrel, which is removed after preparing the front end of the shell and charging it with the mandrel. The installation for planetary rolling of shell ends is located in the off-line charging section and serves both pilger mills, reducing capital costs.

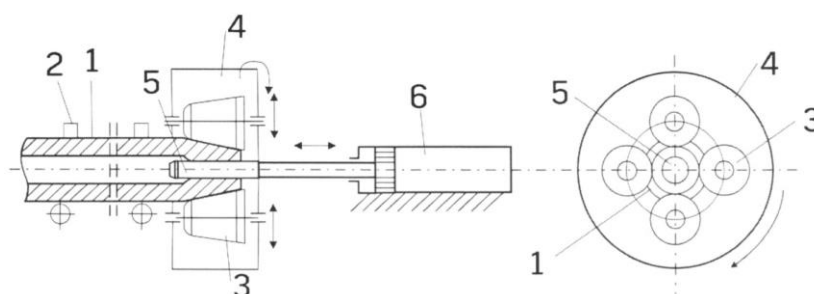


Figure 3 – Preparation of the front end of the shell on a planetary-type rolling machine:
 1 – shell; 2 – shell clamp; 3 – idle compression rolls; 4 – die plate; 5 – mandrel; 6 – mandrel hydraulic drive;

3. Preparation of the front ends of billets before the skew-roll piercing PRM with a three-roll mill using a planetary rolling device was proposed by G.M. Kushchinsky in the late 1960s [18]. A feature of this installation is the simultaneous centering of the billet's front

end during its preparation. G.M. Kushchinsky's research demonstrated the feasibility, possibility, and effectiveness of such billet preparation.

4. Several processes for using planetary rolling in cold deformation of pipes are known. At SE «NDTI»

and NMetAU, in order to expand the assortment in the production of bearing pipes with diameters less than 50 mm, a new process of mandrel-less cold transverse-helix rolling was proposed, performed in a planetary stand with a differential drive. Works [19, 20] in the field of screw rolling on planetary hot- or cold-rolling pipe mills demonstrated the effectiveness of this new production method. The main technological feature of planetary screw rolling mills is the ability to deform the

metal gradually. This is achieved through a special drive arrangement of the mill: the use of a differential gearbox and two main motors (one motor for roll rotation and one for stand rotation). Cold screw rolling was performed on a three-roll planetary mill installed at SE «NDTI» with roll feed α angles of $3^{\circ}30'$ and 7° , and a stand rotation speed of $n_{kn} = 5 \text{ s}^{-1}$ and 10 s^{-1} .

The scheme of the planetary mill is shown in fig. 4.

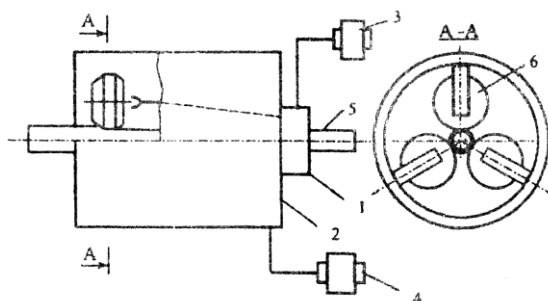


Figure 4 – Planetary screw rolling mill: 1 – central gear of the differential gearbox; 2 – working stand; 3 – roll motor (central gear); 4 – stand motor; 5 – pipe being rolled; 6 – working roll

Pipes with dimensions $32 \times 3,0$ mm, $32 \times 4,0$ mm, and $36,6 \times 4,7$ mm were rolled in a single pass with the following deformation degrees: $32 \times 3,0$ mm – 4–18% relative deformation (ε) and 1,0–5,8 mm absolute deformation (Δd); $32 \times 4,0$ mm – 3–22% relative deformation (ε) and 1,0–7,0 mm absolute deformation (Δd); $36,6 \times 4,7$ mm – 4–18% relative deformation (ε) and 1,5–6,6 mm absolute deformation (Δd).

The productivity of the cold mandrel-less screw rolling process depends on the rotational speed of the planetary stand, the feed angle of the working rolls, and the degree of pipe deformation by diameter, and ranges from 100 to 250 m/h at a total power of 24 kW. The dimensional accuracy of finished bearing pipes is 0,1–0,3 mm by diameter and 4–5% by wall thickness, meeting the requirements of standards for bearing pipes. The surface finish of pipes after cold planetary rolling can reach $Ra = 1 \div 2 \mu\text{m}$. The quality of the internal surface is not deteriorated.

In Japan, rotational pipe calibration has been developed, which provides increased dimensional accuracy, surface quality, and is characterized by low capital and operating costs [21]. The device for rotational calibration contains a housing with rollers that roll along the pipe surface, being installed at a certain angle to the pipe axis. The rollers rotate freely on their axes and are equipped with drives – the rotation of the housing itself provides the drive. The housing moves along the pipe similarly to a nut moving along a thread, as it slides onto the pipe and moves along a spiral trajectory. This ensures that the entire pipe surface is uniformly processed.

By changing the relative angular position of the rollers, the gauge diameter can be adjusted. Each of the two roller housings is mounted on separate carriages. In the second housing, the rollers are installed at an

angle of opposite sign relative to the rollers of the first housing. Both housings rotate in mutually opposite directions, which is necessary to prevent twisting of the pipe in the section between the calibration mill and the welding position. Both carriages are rigidly connected to each other and mounted on guides. The entire assembly of carriages, roller housings, electric motors, and gearboxes can freely move along the guides parallel to the pipe axis (fig. 5). One feature of the rotational calibration method is that the gauge diameter, formed inside the roller housing, is continuously adjustable within the range between the upper and lower limits inherent to that housing. Figure 6 shows the change in diameter corresponding to the variation of the roller installation angle relative to the pipe axis. This allows for a reduction in the tool inventory, as a single pair of roller housings can calibrate several pipe diameters.

The pipe passing through the RSM calibration mill is processed uniformly along its entire length.

Currently, the range of pipes suitable for calibration on the RSM mill is limited to an outer diameter of $30 \div 650$ mm and a wall thickness of $0,8 \div 16$ mm. The RSM calibration mill has the following advantages: high-precision adjustment of pipe tension between the welding machine and the calibration mill; on-the-fly gauge adjustment; the possibility of producing shaped pipes; improved surface roughness of pipes by approximately 30%; quick tool replacement without additional costs; gradual and uniform deformation of the pipe material; a 50% reduction in energy consumption; the possibility of use outside the PRM line; and others.

A known method of continuous cold pipe rolling [22] involves deforming the hollow billet 1 in a gauge formed by grooved rolls 2 on a mandrel 3, and in a consecutively arranged housing 4 that rotates around the rolling axis, where planetary rolling of the billet with idle rolls is carried out (fig. 7).

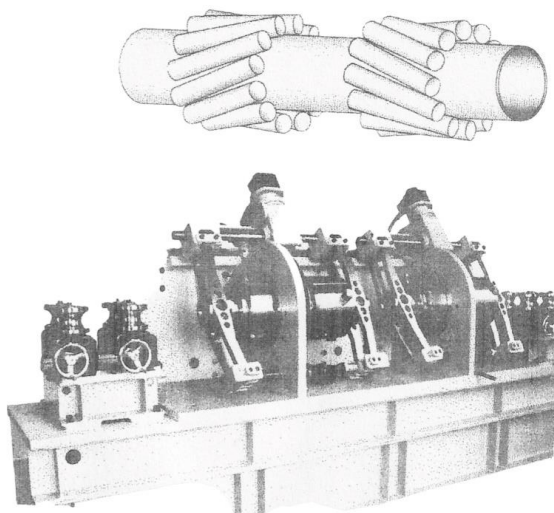


Figure 5 – General view of the installation for rotational pipe calibration

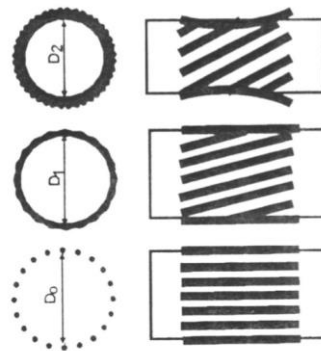


Figure 6 – Diagram of gauge diameter adjustment inside the roller housing

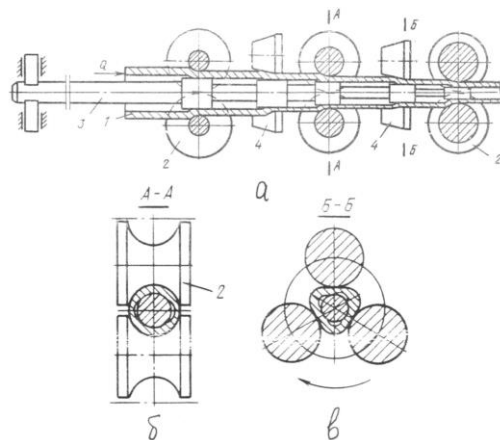


Figure 7 – Scheme of continuous cold pipe rolling [23]:
 a) general view; b and c) cross-sections A–A and B–B, respectively;
 1 – hollow billet; 2 – grooved roll; 3 – mandrel; 4 – housing with idle rolls

Each cross-section of the billet is compressed in both diameter and wall thickness first by the longitudinal rolling rolls, then by the transverse rolling rolls, followed again by the longitudinal rolling rolls, and so on. In this process, the ratio of relative deformations in wall thickness in consecutively arranged gauges – formed by the grooved rolls of the longitudinal rolling and in the planetary housing with idle rolls rotating around the

rolling axis – is $0,5 \div 0,9$. This ensures a reduction in the degree of work hardening and mitigates the higher plastic properties of the metal, i.e., it increases the deformability of the metal and the productivity of the process due to significantly higher elongation coefficients (3,0÷3,8).

Selection of the planetary scheme for rolling the front ends of billets and the parameters of the rollers.

Planetary rolling of the front ends of billets (shells) with rollers can be carried out according to several schemes. Combined rolling with radial feed of the rollers is fairly complex, as it requires an adjustable stop for axial fixation of the billet relative to the rollers. In addition, for radial feed of the rollers during rotation of the roller cassette around the billet, either a collector device or flexible hoses for fluid supply are needed. Therefore, the second rolling scheme is considered more practical, in which the roller cassette moves axially along the billet to deform its front end.

Furthermore, planetary rolling of the billet end can be performed with a varying number of rollers. The number of rollers determines the rotation angle of the cassette, in which the rollers are positioned with the ability to move radially from the initial position to form a conical shape at the billet end.

If one roller is used, then to form the cone it must make one full rotation around the billet plus an additional rotation corresponding to the indentation depth Δh . If two rollers are used in the cassette, positioned diametrically, the cassette must make one full rotation to form the cone. If three rollers are used, positioned at an angle of 120° to each other, the cassette must rotate

by 240° . If four rollers are used, positioned at an angle of 90° to each other, the cassette must rotate by 180° , i.e., half a turn, to form the cone. We adopt a cassette with four rollers.

Determination of deformation tool parameters. These parameters include the diameter and width of the rollers.

The roller diameter is selected by analogy with the selection of rolling roll diameters. As is known, the working diameter of rolling rolls is determined taking into account the allowable bite angle according to the formula

$$D = \frac{\Delta h}{1 - \cos \alpha_3}, \quad (1)$$

where Δh – is the absolute indentation; α_3 – is the bite angle, which should not exceed 30° , we adopt a bite angle of 15° .

The absolute indentation for the minimum billet diameter of $\varnothing 110$ mm, as shown in fig. 8, is $\Delta h = L_K \cdot \operatorname{tg} 5^\circ = 50 \cdot 0,0875 = 4,4$ mm.

The absolute indentation for the maximum billet diameter of $\varnothing 230$ mm, as shown in fig. 8, is $\Delta h = L_K \cdot \operatorname{tg} 5^\circ = 70 \cdot 0,0875 = 6,1$ mm.

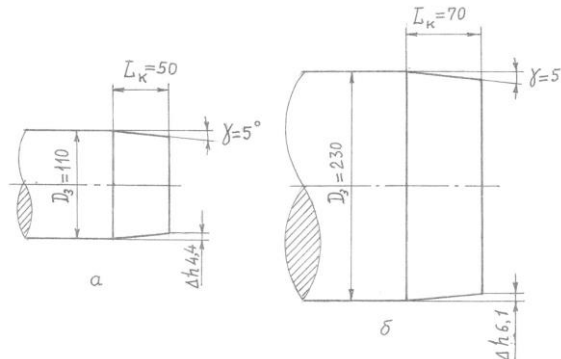


Figure 8 – Billets with profiled front ends:
 a) diameter $\varnothing 110$ mm; b) diameter $\varnothing 230$ mm

Then, according to formula (1), the roller diameter should be:

$$D = \frac{4,4}{1 - 0,9659} \text{ mm}_{min};$$

$$D = \frac{6,1}{1 - 0,9659} \text{ mm}_{max}.$$

– for the minimum billet $\varnothing 110$ mm
 – for the maximum billet $\varnothing 230$ mm

We adopt the roller diameter at the billet end face plane as $D = 200$ mm.

When determining the roller width, it should be taken into account that the end of the cylindrical billet takes a conical shape and elongates in the axial direction during rolling with conical rollers (fig. 9). Let us determine the length L_3 of the billet end, which transitions into the specified cone length L_K . We consider the volumes of two bodies: a cylinder with a diameter of D_3 and a height of L_3 and a truncated cone with a base of D_3 and a height of L_K . From this, we obtain the ratio

$$L_3 = L_K - 2 \cdot \frac{L_K^2 \cdot \operatorname{tg} \gamma}{D_3} + 1,3 \cdot \frac{L_K^3 \cdot \operatorname{tg}^2 \gamma}{D_3^2}.$$

The calculation showed that the third term can be neglected with an error of less than 1%. Based on this, we obtain the formula

$$L_3 = L_K - \frac{2 \cdot L_K^2 \cdot \operatorname{tg} \gamma}{D_3}. \quad (2)$$

From expression (2), the length L_3 for the minimum billet with the initial data: $D_3 = 110$ mm; $L_K = 50$ mm; $\gamma = 5^\circ$ will be equal to $L_3 = 50 - \frac{2 \cdot 50^2 \cdot \operatorname{tg} 5^\circ}{110} = 46$ mm.

From expression (2), the length L_3 for the maximum billet with the initial data: $D_3 = 110$ mm; $L_K = 70$ mm; $\gamma = 5^\circ$ will also be equal to $L_3 = 50 - \frac{2 \cdot 70^2 \cdot \operatorname{tg} 5^\circ}{110} = 66,3$ mm. Then, the roller width is taken from the expression $b_p = L_K + \Delta b_1 + \Delta b_2$. Where Δb_1 is used to position the billet relative to the rollers before the start of rolling. We adopt initial approximate values Δb_1 and Δb_2 as 15 mm. Consequently, the roller width will be $b_p = L_K + 30$.

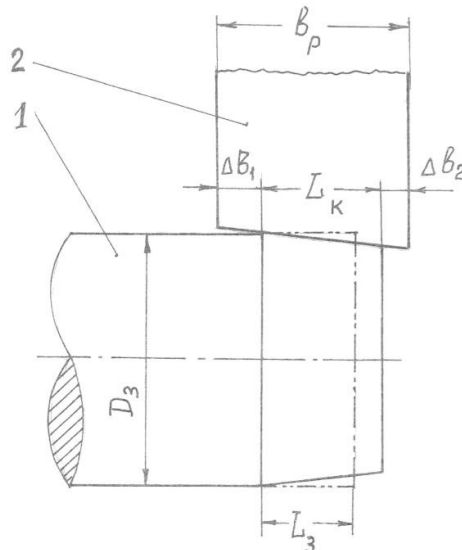


Figure 9 – Diagram of roller contact with the billet at the moment of indentation completion: 1 – billet; 2 – roller

Determination of the forces acting on the roller during the rolling process. The forces acting during the planetary rolling process are determined at the moment of maximum roller penetration into the billet. Fig. 10 shows the force diagram acting on a stationary billet from the idle roller when it is inserted by a distance Δh and the roller cassette is rotated by an angle of 90° counterclockwise. The diagram shows the minimum billet with a diameter of $\varnothing 110$ mm and a roller of $\varnothing 200$ mm. The magnitude Δh is maximal at the billet's end face and decreases to zero at the point where the billet first contacts the roller. The action of the billet on the roller can be represented as a single resultant force P ,

applied at point A, in the middle of the contact arc CD . If the friction forces in the roller trunnions are neglected, this resultant must pass through the roller axis – point O_1 . When friction in the roller trunnions is considered, the direction of the resultant force P changes so that it passes along the tangent to the friction circle. Then, the torque required to rotate the roller is

$$M_p = P \cdot \mu \cdot \frac{d}{2} = P \cdot \rho, \quad (3)$$

where: $\rho = \frac{\mu \cdot d}{2}$ – radius of the friction circle; μ – coefficient of friction in the roller trunnions; d – diameter of the roller trunnions.

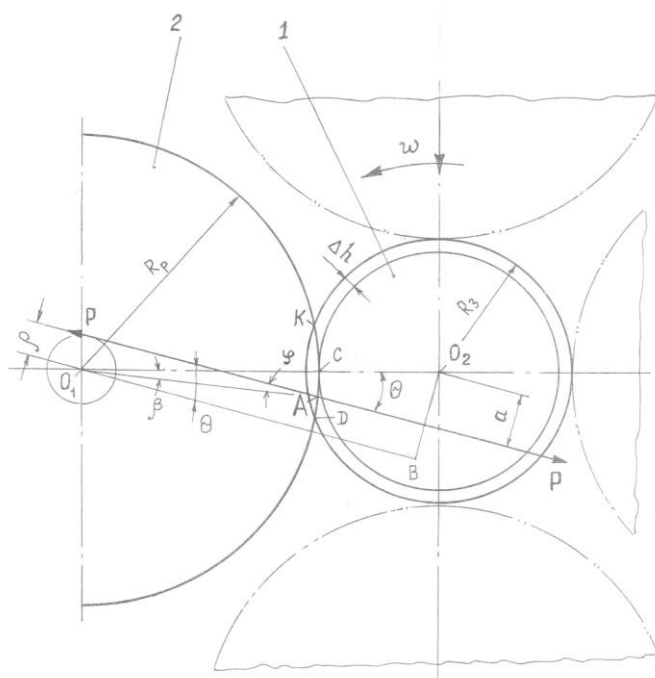


Figure 10 – Diagram of the force interaction between the roller and the billet at the moment of indentation completion: 1 – billet; 2 – roller.

The force exerted by the roller on the billet, based on equilibrium conditions, lies on the same line as force P and generates a torque that tends to rotate the billet counterclockwise.

$$M_3 = P \cdot a, \quad (4)$$

where $a = BO_2 - \rho$; $BO_2 = (R_p + R_3 - \Delta h) \cdot \sin \theta$.

From triangle ACO_1 it follows that $\theta = \beta + \varphi$. The angle β is determined by the point A of application of the resultant P on the roller, and the angle φ can be found from the relation $\sin \varphi = \frac{2 \cdot \rho}{D_p}$. The lever arm a of the force P can now be determined from the equation:

$$a = (R_p + R_3 - \Delta h) \cdot \sin(\beta + \varphi) - \rho. \quad (5)$$

Substituting this value of a into expression (4), we obtain the moment acting on the billet taking into account the frictional forces in the roller trunnions. We estimate the magnitude of the force P as the resultant of the normal pressure forces acting over the contact arc CD of the roller with the billet when the roller is inserted by an amount Δh . We assume that the mean

value of the normal pressure equals p and is uniformly distributed over the contact arc CD and over the contact patch between the roller and the billet. The contact patch is represented as an isosceles triangle whose base is the chord of the contact arc CD and whose height is L_K . We use the slip-line method and consider a plane problem. We choose the indentation speed of the rollers such that indentation by the prescribed amount Δh occurs during one quarter turn of the roller cassette around the billet. Obviously, in this position the indentation force of the rollers reaches its maximum. This position is shown in Fig. 11, where a simplified slip-line field is adopted consisting of two straight lines AC and $A'C'$. On the contact surfaces AB and $A'B'$ a constant average pressure p , directed perpendicular to the billet axis and parallel to the roller velocity v_p , directed along the radius O_1A (fig. 11). The velocity v_p is determined from the relation

$$v_p' = v_p \cdot \sin \beta,$$

where v_p – the tangential velocity of the center of the roller axis O_1 during the cassette's rotation about the workpiece.

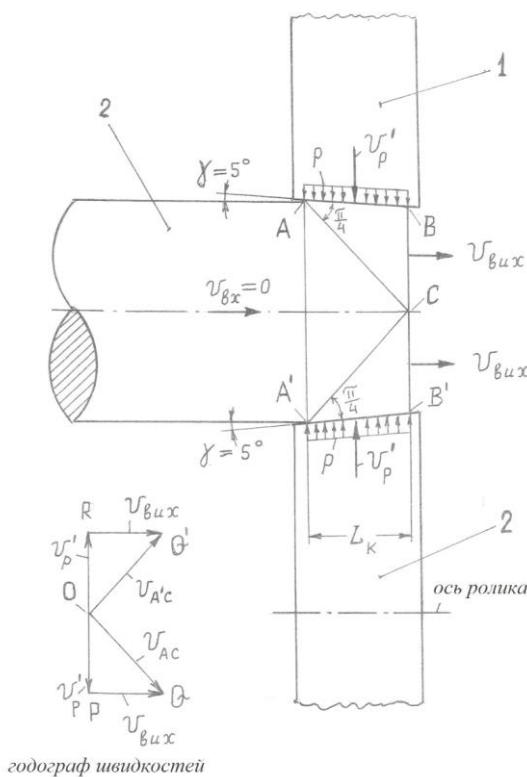


Figure 11 – Slip-line field at maximum indentation of two diametrically opposed rollers and velocity hodograph:
 1 – roller; 2 – billet

The error δ , which arises from replacing the pressure normal to the surface AB with the pressure p , perpendicular to the workpiece axis, is estimated as negligibly small (at $\gamma = 5^\circ$), namely:

$$\delta = \frac{\Delta p}{P_N} \cdot 100\% = \frac{P_N - P_N \cdot \cos \gamma}{P_N} \cdot 100\% = 0,38\%.$$

The construction of the slip velocity hodograph is carried out as follows. From the pole O (fig. 11) to an arbitrary scale, we lay off the velocities v_p of the rollers relative to the center of the workpiece (more precisely, to points A and A') OP and OR . In each deformation zone ABC and $A'B'C'$ these velocities have two

components: OQ along AC and OQ' along $A'C$, as well as PQ and RQ – the velocities of the metal exiting the deformation zone. The upper-limit specific load p is calculated according to Johnson's method [23, p. 218] using the equation

$$p \cdot AB = \frac{2 \cdot \sigma_s}{\sqrt{3}} \cdot \int_s \frac{v_{CK}}{v_p} ds = \frac{2 \cdot \sigma_s}{\sqrt{3}} \cdot \frac{AC \cdot OQ}{v_p}. \quad (6)$$

From where, we get

$$p = \frac{2 \cdot \sigma_s}{\sqrt{3}} \cdot \frac{AC \cdot OQ}{AB \cdot OP}. \quad (7)$$

The measurements of the segments included in formula (7) on the drawing (Fig. 11) yielded the following values: $AC = 37$ mm; $OQ = 26,5$ mm; $AB = 26$ mm; $OP = 20$ mm. Substituting the obtained values into formula (7), we get

$$p = \frac{2}{\sqrt{3}} \cdot \frac{37 \cdot 26,5}{26 \cdot 20} \cdot \sigma_s = 2,18 \cdot \sigma_s.$$

To determine the yield strength σ_s of the steel, it is necessary to know the degree and rate of deformation. The degree of deformation ε is estimated by analogy with cylinder upsetting. In our case, it is not upsetting, but the elongation of the workpiece end from length L_3 to length L_K .

Thus, the degree of deformation during rolling is determined as follows:

$$\begin{aligned} & \text{– for the minimum workpiece } \varnothing 110 \text{ mm } \varepsilon = \frac{L_K - L_3}{L_3} \\ & 100\% = \frac{50 - 46}{46} \cdot 100\% = 8,7\%; \\ & \text{– for the maximum workpiece } \varnothing 230 \text{ mm } \varepsilon = \frac{L_K - L_3}{L_3} \\ & 100\% = \frac{70 - 66,3}{66,3} \cdot 100\% = 5,6\%. \end{aligned}$$

The deformation rate $u = \varepsilon/t$, where t – is the deformation time, depends on the angular velocity ω of the roller cassette. Thus, if the cassette rotates at a speed of $n = 60 \text{ min}^{-1}$ ($\omega = \frac{\pi \cdot n}{30} = 6,28 \text{ s}^{-1}$), the time

for the cassette to turn through an angle of 90° will be $= 0,25 \text{ s}$.

Therefore, the deformation rate of the workpiece end during roller finishing will be:

$$\begin{aligned} & \text{– for the minimum workpiece } \varnothing 110 \text{ mm } u = \frac{0,087}{0,25} = \\ & 0,35 \text{ s}^{-1}; \\ & \text{– for the maximum workpiece } \varnothing 230 \text{ mm } u = \frac{0,056}{0,25} = \\ & 0,22 \text{ s}^{-1}. \end{aligned}$$

As an example, we consider a workpiece made of steel 45 at a temperature of 1200°C .

We determine the yield strength of this steel using the method of thermomechanical coefficients [24, p. 212]:

$$\sigma_s = \sigma_0 \cdot k_\varepsilon \cdot k_u \cdot k_T \quad (8)$$

where $\sigma_0 = 86 \text{ MPa}$ – the baseline value of deformation resistance [24, p. 212]; $k_\varepsilon = 0,93$ – the step coefficient for the minimum workpiece; $k_\varepsilon = 0,95$ – the step coefficient for the maximum workpiece; $k_u = 0,62$ the velocity coefficient for the minimum workpiece; $k_u = 0,57$ the velocity coefficient for the maximum workpiece; $k_T = 0,58$ the temperature coefficient for the workpieces.

Then, the yield strength will be:

$$\begin{aligned} & \text{– for the minimum workpiece } \varnothing 110 \text{ mm } \sigma_s = 86 \cdot \\ & 0,93 \cdot 0,62 \cdot 0,58 = 28,76 \text{ MPa}; \\ & \text{– for the maximum workpiece } \varnothing 230 \text{ mm } \sigma_s = 86 \cdot \\ & 0,95 \cdot 0,57 \cdot 0,58 = 27 \text{ MPa} \end{aligned}$$

The value of the specific pressure p on sections AB and $A'B'$ (fig. 11):

$$\begin{aligned} & \text{– for the minimum workpiece } \varnothing 110 \text{ mm } p = 2,18 \cdot \\ & 28,76 \approx 62,7 \text{ MPa}; \\ & \text{– for the maximum workpiece } \varnothing 230 \text{ mm } p = 2,18 \cdot \\ & 27 \approx 60 \text{ MPa}. \end{aligned}$$

For the maximum workpiece, the specific pressure p on sections AB i $A'B'$ has also been determined using Johnson's method in the form $p = 2,22 \cdot \sigma_s$. Due to its identity with the minimum workpiece, the determination itself is not presented here. To determine the force P it is necessary to know the contact area of the roller with the workpiece, which is calculated using the formula:

$$F_K = \frac{1}{4} \cdot L_{KD} \cdot L_K, \quad (9)$$

where L_{KD} – the length of the common chord at the intersection of the workpiece and roller circles.

Let us determine the chord length L_{KD} . According to fig. 12, we have two equations for the chord:

$$\begin{aligned} L_{KD} &= 2 \cdot R_p \cdot \sin \gamma_1; \\ L_{KD} &= 2 \cdot R_3 \cdot \sin \gamma_2. \end{aligned} \quad (10)$$

From where, we have one equation: $R_p \cdot \sin \gamma_1 - R_3 \cdot \sin \gamma_2 = 0$. The second equation is obtained by expressing the distance between the axes of the roller and the workpiece as $R_p \cdot \cos \gamma_1 + R_3 \cdot \cos \gamma_2 = R_p + R_3 - \Delta h$. We thus have a system of two equations with two unknowns γ_1 and γ_2 :

$$\begin{aligned} R_p \cdot \sin \gamma_1 - R_3 \cdot \sin \gamma_2 &= 0; \\ R_p \cdot \cos \gamma_1 + R_3 \cdot \cos \gamma_2 &= R_p + R_3 - \Delta h. \end{aligned} \quad (11)$$

Solving this system of equations leads to the following expression:

$$\sqrt{1 - \left(\frac{R_p}{R_3}\right)^2 + \left(\frac{R_p}{R_3}\right)^2 \cdot \cos^2 \gamma_1} + \frac{R_p}{R_3} \cdot \cos \gamma_1 = \frac{R_p}{R_3} + 1 - \frac{\Delta h}{R_3}. \quad (12)$$

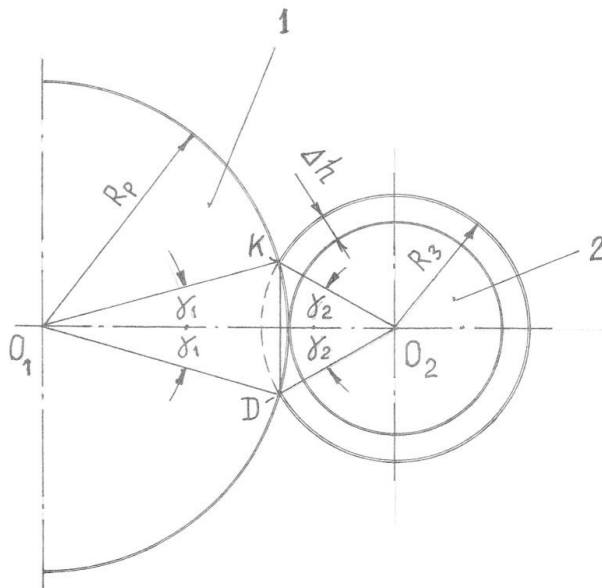


Figure 12 – Diagram for determining the length of the common chord of the roller and workpiece:
 1 – roller; 2 – workpiece

We solve equation (12) for the minimum workpiece with respect to γ_1 using the following values of the parameters involved: $\frac{R_p}{R_3} = \frac{100}{55} = 1,818$; $\left(\frac{R_p}{R_3}\right)^2 = 1,818^2 = 3,305$; $\Delta h = 4,4$ mm; $\frac{\Delta h}{R_3} = \frac{4,4}{55} = 0,08$. As a result of solving equation (12), we obtain $\cos \gamma_1 = 0,984$, from which $\gamma_1 = 10^\circ 20'$ follows.

We solve equation (12) for the maximum workpiece with respect to γ_1 using the following values of the parameters involved: $\frac{R_p}{R_3} = \frac{100}{115} = 0,87$; $\left(\frac{R_p}{R_3}\right)^2 = 0,87^2 = 0,756$; $\Delta h = 6,1$ mm; $\frac{\Delta h}{R_3} = \frac{6,1}{115} = 0,053$. As a result of solving equation (12), we obtain $\cos \gamma_1 = 0,967$, from which $\gamma_1 = 14^\circ 44'$ follows.

Thus, the chord length according to equation (10) is:

- for the minimum workpiece $\varnothing 110$ mm $L_{KD} = 2 \cdot 100 \cdot \sin 10^\circ 20' \approx 36$ mm;
- for the maximum workpiece $\varnothing 230$ mm $L_{KD} = 2 \cdot 100 \cdot \sin 14^\circ 44' \approx 51$ mm.

Then, the contact area of the roller with the workpiece, according to formula (9), will be:

- for the minimum workpiece $\varnothing 110$ mm $F_k = 0,25 \cdot 36 \cdot 50 = 450$ mm²;
- for the maximum workpiece $\varnothing 230$ mm $F_k = 0,25 \cdot 51 \cdot 70 = 892,5$ mm².

The force \mathbf{F} will be:

- for the minimum workpiece $\varnothing 110$ mm $P = p \cdot F_k = 62,7 \cdot 10^6 \cdot 450 \cdot 10^{-6} = 28215$ N = 28,2 kN;
- for the maximum workpiece $\varnothing 230$ mm $P = p \cdot F_k = 60 \cdot 10^6 \cdot 892,5 \cdot 10^{-6} = 53550$ N = 53,55 kN.

The torque required to rotate the roller during finishing is determined using formula (3) at $\mu = 0,1$ and $d = 0,1$ m:

- for the minimum workpiece $\varnothing 110$ mm $M_p = 28215 \cdot 0,1 \cdot \frac{0,1}{2} = 141,07$ N · m;
- for the maximum workpiece $\varnothing 230$ mm $M_p = 28215 \cdot 0,1 \cdot \frac{0,1}{2} = 267,75$ N · m.

We determine the angle:

$$\varphi = \arcsin \frac{2 \cdot \rho}{D_p} = \arcsin \frac{2 \cdot 5}{200} = \arcsin 0,05,$$

where $\rho = \frac{\mu \cdot d}{2} = \frac{0,1 \cdot 100}{2} = 5$ mm – the radius of the friction circle.

Thus, the angle $\varphi \approx 2^\circ 50'$.

From Fig. 10, it can be seen that the angle $\beta = \frac{\gamma_1}{2}$. Therefore, for the minimum workpiece $\varnothing 110$ mm, the angle $\beta = 5^\circ 10'$, and for the maximum workpiece $\varnothing 230$ mm, the angle $\beta = 7^\circ 22'$.

Next, using formula (5), we determine the lever arm of the force P :

- for the minimum workpiece $\varnothing 110$ mm $a = (100 + 55 - 4,4) \times \sin(5^\circ 10' + 2^\circ 50') - 5 = 16$ mm;
- for the maximum workpiece $\varnothing 230$ mm $a = (100 + 115 - 6,1) \times \sin(7^\circ 22' + 2^\circ 50') - 5 = 32$ mm.

Using formula (4), we calculate the torque tending to rotate the workpiece counterclockwise:

- for the minimum workpiece $\varnothing 110$ mm $M_3 = 28215 \cdot 16 \cdot 10^{-3} = 451,44$ N · m;
- for the maximum workpiece $\varnothing 230$ mm $M_3 = 53550 \cdot 32 \cdot 10^{-3} = 1713,6$ N · m.

Thus, the total torque acting on the stationary workpiece from the four rollers is:

- for the minimum workpiece $\varnothing 110$ mm $\sum M_3 = 4 \cdot 451,44 \approx 1806$ N · m;
- for the maximum workpiece $\varnothing 230$ mm $\sum M_3 = 4 \cdot 1713,6 \approx 6854$ N · m.

To rotate the cassette with four rollers, without accounting for friction losses in the drive, the previously found total torque on the rollers is required. Then, the power needed to rotate the rollers (also without considering the drive efficiency) will be:

– for the minimum workpiece $\varnothing 110$ mm $N = \sum M_3 \cdot \omega_k = 1806 \cdot 6,28 = 11342$ W = 11,34 kW;

– for the maximum workpiece $\varnothing 230$ mm $N = \sum M_3 \cdot \omega_k = 6854 \cdot 6,28 = 43043$ W = 43,04 kW.

Preparation of the front ends of shells on a finishing (rolling) machine. The schematic of the planetary finishing of the front end of a shell on a mandrel is shown in fig. 13. In this process, the shell 1 is stationary and secured against rotation. Four cylindrical rollers 2 are positioned in diametrically opposite planes in pairs, with the ability to move along the radii of the shell cross-section. Thus, the axes of the forming rollers are parallel to the axis of the shell. The movement of each roller is driven by a hydraulic cylinder 3, mounted in the housing 4. The housing can rotate on a bearing support 5 and has a gear wheel 6, which receives rotation

from the drive pinion 7. The shell 1 is mounted on the mandrel 8 to a specified distance corresponding to the length of the deforming rollers 2. The mandrel is secured against axial displacement. A hydraulic manifold 9 is installed on the mandrel, which conveys working fluid from the stationary mandrel to the rotating housing 4, and then to each hydraulic cylinder and back to the drain.

The force of the rollers' penetration into the shell wall, as well as the torque applied to housing 4, can be varied over a wide range depending on the radial feed of the rollers per one rotation of the housing 4. By analogy with the cutting force on lathes, this force can be determined experimentally. Synchronization of the gradual movement of the rollers toward the shell center can be achieved by known hydraulic methods (adjustable throttles, use of false rods, discrete hydraulic drives, etc.).

The penetration of the rollers into the shell wall can be limited by displacement sensors on the rods, force sensors, or torque sensors.

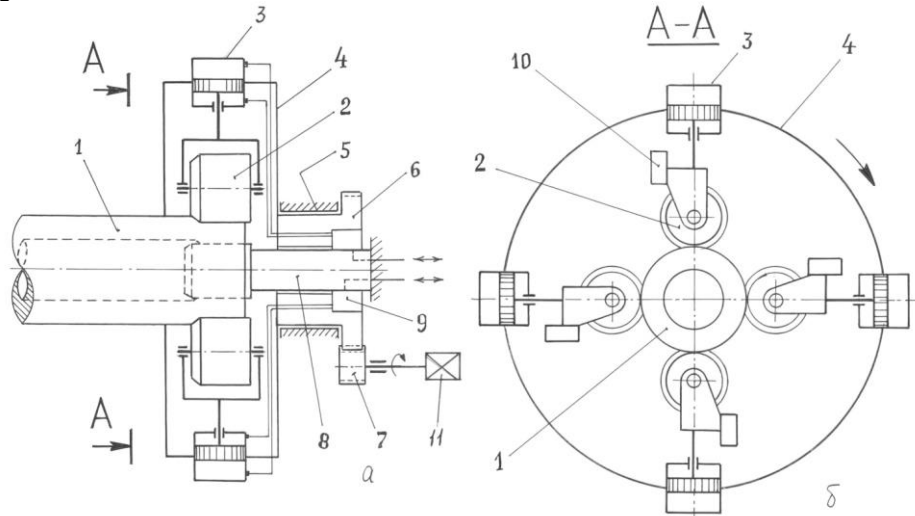


Figure 13 – Diagram of planetary finishing of the front end of a shell:
 a) main view; b) cross-section A-A in the main view;
 1 – shell; 2 – forming roller; 3 – hydraulic cylinder; 4 – housing; 5 – bearing support; 6 – gear wheel; 7 – drive pinion; 8 – mandrel; 9 – hydraulic manifold; 10 – support; 11 – rotation drive

The rollers are cylindrical in shape and move synchronously toward the center of the shell. There is a radial clearance between the shell and the mandrel (fig. 14) $\Delta r = \frac{(d_e - D_{onp})}{2}$. Fig. 14 shows the front end of the shell in a diametral section at the moment of completion of reduction, when the chosen radial clearance Δr , is set, the deforming rollers have penetrated the shell wall by ΔR , and the contact length l of the rollers with the shell has increased by Δl . The dashed line in fig. 14 shows the initial position of the shell end relative to the rollers and mandrel.

As a result of the reduction, the volume of metal in a ring with cross-section $ABCD$ is deformed into a ring with cross-section $A'B'C'D'$. The volume of the ring $ABCD$ can be determined using the expression:

$$V_{ABCD} = F_m \cdot l = \frac{\pi}{4} \cdot (D_e^2 - d_e^2) \cdot l, \quad (13)$$

where F_m – the area of the flat annular cross-section AD ; D_e – the outer diameter of the shell; d_e – the inner diameter of the shell.

The volume of the ring $A'B'C'D'$ can be determined using the expression:

$$V_{A'B'C'D'} = F_m' \cdot (l + \Delta l) = \frac{\pi}{4} \cdot [(D_e - 2 \cdot \Delta R)^2 - D_{onp}^2] \cdot (l + \Delta l), \quad (14)$$

where F_m' – the area of the flat annular cross-section $A'D'$.

Equating expression (13) and expression (14), and dividing by 1, we obtain:

$$D_e^2 - d_e^2 = [(D_e - 2 \cdot \Delta R)^2 - D_{onp}^2] \cdot \left(1 + \frac{\Delta l}{l}\right). \quad (15)$$

We have one equation with two unknowns, ΔR and Δl .

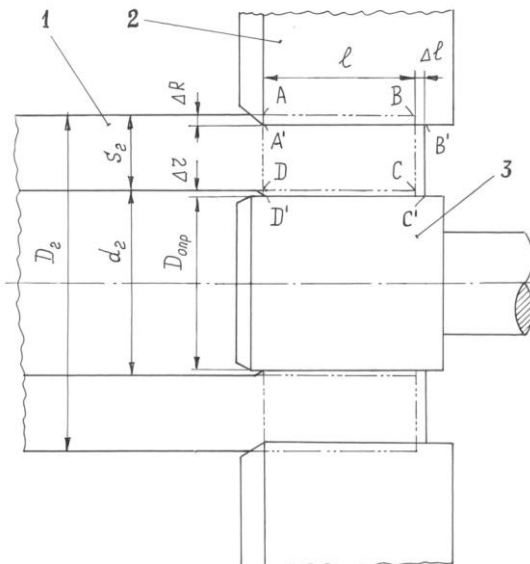


Figure 14 – Finishing of the shell end with rollers on a mandrel (longitudinal section):
 1 – shell; 2 – forming roller; 3 – mandrel

The second equation is obtained from the incompressibility condition:

$$\varepsilon_l + \varepsilon_R + \varepsilon_t = 0,$$

where $\varepsilon_l = \frac{\Delta l}{l}$ – relative elongation of the shell end (positive sign); $\varepsilon_R = \frac{2 \cdot \Delta R}{D_e}$ – relative reduction of the shell radius (negative sign); $\varepsilon_t = \frac{[\pi \cdot D_e - \pi \cdot (D_e - 2 \cdot \Delta R)]}{(\pi \cdot D_e)} = \frac{2 \cdot \Delta R}{D_e}$ – relative deformation in the tangential direction (negative sign).

Thus, the second equation is:

$$\frac{\Delta l}{l} - \frac{4 \cdot \Delta R}{D_e} = 0. \quad (16)$$

Solving equations (15) and (16) simultaneously with respect to ΔR , we obtain:

$$D_e^2 - d_e^2 = [(D_e - 2 \cdot \Delta R)^2 - D_{onp}^2] \cdot \left(1 + \frac{4 \cdot \Delta R}{D_e}\right). \quad (17)$$

Equation (17) is cubic with respect to ΔR . Therefore, it is expedient to proceed to a numerical solution. Substituting the following initial data into equation (17): $D_e = 320$ mm, $d_e = 170$ mm, $D_{onp} = 164$ mm, $l = 140$ mm.

We obtain the cubic expression:

$$0,05 \cdot \Delta R^3 - 12 \cdot \Delta R^2 - 336,2 \cdot \Delta R + 2004 = 0.$$

By substituting values of ΔR we find the value of $\Delta R = 5,06$ mm, that satisfies this equation.

From equation (16), we obtain $\Delta l = 8,86$ mm.

The thinning of the shell wall occurs by an amount of

$$\Delta S = \Delta R - \Delta r = 5,06 - 3 = 2,06 \text{ mm}.$$

Conclusions.

1. One of the main reserves for further increasing productivity, saving material, and improving the accuracy of geometric dimensions in the production of hot-rolled seamless pipes is the use of variable deformation modes across the wall thickness.

2. The method of transferring part of the deformation from the main pass to the preceding pass has been developed, which significantly improves rolling conditions in the main pass and enhances its performance indicators.

3. Examples of performing additional operations on different passes of the rolling stand have been considered, demonstrating their high efficiency.

4. Planetary rolling processes used in pipe rolling production for designing the method of preparing the front ends of shells have been examined.

5. Using the slip-line method, the forces acting on idle rolls during transverse planetary finishing of the shell end, as well as the torque and power of finishing, have been determined.

6. The process of preparing the front end of the shell by reducing it without wall-thickness compression through transverse planetary finishing with idle rolls has been analyzed, and the thinning of the shell wall at the front end has been determined analytically.

7. The process of transverse planetary finishing for preparing the ends of billets, shells, and pipes is promising and requires further research and development.

8. The results of this work can be used when selecting a rational method for preparing metal for rolling, taking into account the technology at a specific rolling stand.

References

1. Velichko, A. G., Bolshakova, V. I., & Balakina, V. F., (Eds.) (2015). *Sovershenstvovanie proizvodstva stali, trub i zheleznodorozhnyh koles : kollektiv. monografiya: Ekonomika*.
2. Mironov, Yu. M., & Ratner, A. G. (1983). Opty i perspektivy ispolzovaniya peremennyyh rezhimov goryachej deformacii pri proizvodstve besshovnyh trub. *Novye tehnologii proizvodstva stalnyh trub*.
3. Safyanov, A. V., & Potapov I. N. (1974). Issledovanie i sovershenstvovanie proshivki v neustanovivshisya rezhimah. *Stal*, (7), 635-638.
4. Safyanov, A. V., & Potapov, I. N. (1976). Sovershenstvovanie proshivki trubnoj zagotovki v neustanovivshisya rezhimah. *Stal*, (12), 1115-1117.
5. Emec, V. I., & Lapin, L. I. (1987). Osobennosti formoizmeneniya zadnih koncov gilz pri vintovoj proshivke v stane s gribovidnymi valkami. *Sovershenstvovanie processov obrabotki metallov davleniem*, 106-109.
6. Finagin, M., Rodin, N. M., & Podkustov, V. P. A.s. 1407597 SSSR, MKI B21B19/04. Sposob podgotovki zagotovki k vintovoj proshivke. Bulletin. No. 25.
7. Kartushov, B. P., & Kuryatnikov, A. V. (1980). Proshivka profilirovannyh trubnyh zagotovok na stanah vintovoj prokatki /. *Byulleten CIIN ChM*, (19), 43-44.
8. Balakin, V. F., & Ugryumov Yu. D. (2012). Metody podgotovki perednih koncov gilz pered prokatkoj trub / *Teoriya i praktika metallurgii*, (1-2), 16-24.
9. Tartakovskij, B. I. (2010). Geometricheskie, kinematicheskie i silovye parametry processa pri peremeshenii opravki v proshivnom stane. *Proizvodstvo prokata*, (12), 28-36.
10. Hanin, M. I. (2002). Tehnologiya prokatki tonkostennyyh trub povyshennoj tochnosti na aggregate s avtomaticheskim stanom s ispolzovaniem nestacionarnyh rezhimov deformacii pri proshivke. *Metallurgicheskaya i gornorudnaya promyshlennost*, (8-9), 361-363.
11. Chernyavskij A.A., Berezovskij V.V., & Ugryumov Yu.D. (1987). Ekonomiya metalla pri proizvodstve trub neftyanogo sortametnta. *Metallurgiya*, 304.
12. Danchenko, V. N., & Grinev, A. F. (1975). Podgotovka perednih koncov trub pered reducirovaniem. *Metallurgicheskaya i gornorudnaya promyshlennost*, (4), 31-33.
13. Gulyaev, G. N., & Nechiporenko, A. I. (1977). Razrabotka i osvoenie novoj tehnologii prokatki i reducirovaniya trub s utonennymi koncami. *Stal*, (8), 735-739.
14. Gulyaev, G. N., Ratner, A. G., & Zhurba, A. S. (1989) Uluchshenie kachestva trub i ekonomiya metalla pri reducirovani. *Tehnika*, 144.
15. Hanin, M. I. (2013). Rezhimy proshivki, obosnovyyayushie snizhenie prodolnoj raznostennosti trub na agregatah s korotkoopravochnymi stanami. *Metallurgicheskaya i gornorudnaya promyshlennost*, (2), 48-50.
16. Mortelatici, By Luca, & Ricei, Mario. (1996). *Steel Times*, 9(224), 299-302.
17. Balakin, V. F., & Stasevskij, S. L. (2018). Proektirovanie novyh tehnologicheskikh processov podgotovki perednih koncov gilz k piligrimovoj prokatke. *Metallurgicheskaya i gornorudnaya promyshlennost*, 2, 45-51.
18. Bibik, G. A., Druyan, V. M. A.s. 286940 SSSR, MKI B21B19/00. Ustroystvo dlya podgotovki konca zagotovki pered prokatkoj / Ya.L.Vatkin, zayavl. 25.11.69; opubl. 19.11.70, Bulletin No.35.
19. Popov, M. V., & Hanin M. I. (1992). Poluchenie holodnodeformirovannyh podshipnikovyh trub putem reducirovaniya v planetarnoj kleti poperechno-vintovoj prokatki. *Stal*, 11. 59-61.
20. Sposob vyrobnytstva trub : pat. 54610 Ukraina: MPK B21B23/00, B21B19/00, B21B21/00.; zaiavl. 13.02.2001; opubl. 17.03.2003, Bulletin No.3/2003.
21. Nurmahmetov, F. D. (2007). Rotacionnaya kalibrovka na truboprokatnom aggregate. *Novosti chernoj metallurgii za rubezhom*, 2, 68-71.
22. A.s. 1222338 SSSR, MKI B21B17/04, B21B23/00. Sposob nepreryvnoj holodnoj prokatki trub / M.V.Popov, O.A.Plyackovskij, A.A.Fotov i dr.; zayavl. 20.09.84; opubl. 07.04.86, Bulletin No.13.
23. Tomsen, E., Yang Ch., & Kabayashi, Sh. (1969). *Mehanika plasticheskikh deformacij pri obrabotke metallov. Mashinostroenie*.
24. Zyuzin, V. I., Brovman, M. Ya., & Melnikov, A. F. (1964). *Soprotivlenie deformacii stalej pri goryachej prokatke*. Metallurgiya.

Надіслано до редакції / Received: 05.03.2025
Прийнято до друку / Accepted: 30.05.2025